Insight into the corrosion inhibition and adsorption behavior of synthetic pyrazole surfactants as an efficient inhibitor for carbon steel in 1.0 mol/L HCl solutions

M. Alfakeer,[1]* Tasnem Al-Habal,[2] Refat El-Sayed,[3,4] Reda Abdel-Hameed[5,6] and M. Abdallah[2,3]**

[1]Chemistry Department, Faculty of Science, Princess Nourah bint Abdulrahman University, Riyadh, Saudi Arabia
[2]Chemistry Department, Faculty of Applied Science, Umm Al-Qura University, Makkah, Saudi Arabia
[3]Chemistry Department, Faculty of Science, Benha University, Benha, Egypt
[4]Chemistry Department University College in Al-Jamoum, Umm Al-Qura University, Makkah, Saudi Arabia
[5]Chemistry Department, Faculty of Science, Al-Azhar Univ., 11884 Egypt
[6]Basic Science Department, Preparatory Year, University of Hail, Hail, 1560, Saudi Arabia
*E-mail: *metwally555@yahoo.com; **msalonazi@pnu.edu*

Abstract

Two nonionic surfactants (NI Surf.) compounds derived from pyrazole were synthesized and inspected as inhibitors for corrosion of C-steel (CSt) in 1 mol/L HCl solution utilizing weight reduction (*WR*), potentiodynamic polarization (PDP) and electrochemical impedance spectroscopic (EIS) methods. The chemical compositions of the synthetic NI Surf. were proven by IR, ^{1}H and ^{13}C NMR. The corrosion and surface properties confirm the inhibitory effect of the NI Surf. compounds. The percentage of inhibitory efficacy (%) increases with increasing NI Surf concentration, and with decreasing temperature. PDP method has proven that the NI Surf. **I** and **II** act as mixed inhibitors. The maximum %η was found to be 90.41% for the compound **I** and 91.45% for compound **II** at a concentration of 500 ppm at 292 K temperature using PDP measurements. The higher %η of compound **II** is related to its chemical structure and the presence of more adsorption centers. The inhibition was demonstrated by its spontaneous adsorption on the CSt surface owing to the Freundlich isotherms. There is a clear agreement between the % values that were assigned from the different techniques.

Received: June 20, 2023. Published: November 20, 2023 doi: 10.17675/2305-6894-2023-12-4-31

Keywords: *C-steel, nonionic surfactant, corrosion, inhibitors, adsorption, surface activity*.

1. Introduction

Carbon steel (CSt) is utilized in numerous strategic industries and it has multiple advantages such as its economic cost is low and stellar mechanical properties. Therefore, it is used in

many strategic industries such as building and construction operations, nuclear fuel power stations, mining, oil pipelines, and other uses [1, 2]. Usually, strong acids such as HCl solutions are employed for cleaning, descaling, and pickling of steel but it corrodes the steel. Most researchers try to solve this problem in several ways, the chief among them is the use of corrosion inhibitors [3–5]. Organic compounds contain heteroatoms, unsaturated bonds, and aromatic cycles that are used to reduce the aggressive attack of the acids [6–15]. The inhibitory impact of these molecules relied on certain factors such as the composition and the charge allocation on the molecule, the existence of some adsorption centers, and the kind of interaction between the molecule and the steel surface [16–20]. The formation of the adsorbed layer isolates the steel from the corrosive medium and hence decreases the corrosion rate.

From previous studies, it was found that organic compounds reduce corrosion rate and give significant inhibition efficiency, however, the majority of them are economically useless because they are expensive, toxic, and not environmentally friendly. To avoid these shortcomings, scientists tended to use nonionic surfactant compounds, which are economically profitable because they are cheap, safe, not harmful to health and easy to prepare. Previous studies have shown that they give high efficiency of inhibition due to the vigor adsorption of these surfactants on the steel surface [21–28]. The previous work of Abdallah *et al*., [29] tested two nonionic surfactants that were obtained by oxadiazole and thiadiazol derivatives as inhibitors for the dissolution of CSt in 1 mol/L HCl. The two inhibitors are inhibiting the corrosion with good efficacy by their adsorption on the CSt surface.

The main objective of this manuscript is to estimate the corrosion inhibition of CSt in 1 mol/L HCl solutions using synthetic nonionic surfactants (NI Surf.) derived from pyrazole. The inhibitory potency of investigated molecules was evaluated using chemical and electrochemical methods. The influence of elevated temperature and calculation of thermodynamic functions and the type of the adsorption isotherm were determined and interpreted.

2. Experimental

2.1. Corrosion measurements

All the corrosion experiments were performed on CSt having the chemical composition (weight percent %): 0.09 C, 1.27 Mn, 0.01 S, 0.01 P, 0.202 Si, 0.04Al, 0.05V, 0.21 Ni, 0.01Cr and the remaining is Fe. All the solutions were prepared using twice distilled water. For the weight reduction (*WR*) method a specimen with dimensions of $1\times1.79\times0.18$ cm^3 was utilized. For the potentiodynamic polarization (PDP) and electrochemical impedance spectroscopic (EIS) technique, the CSt rod submerged in Alardite with an exposed area of 0.37 cm^2 was applied. Before any measurement, the C-steel specimens or rods were abraded with sandpaper, degreased with solvent, and washed with distilled water.

In this study, two NI Surf. compounds were prepared as follows: Inhibitor stock solution (1000 ppm) was made by dissolving it in a 20% volume of ethyl alcohol in water and the needed concentration of inhibitor was prepared by dilution using bi-distilled water and when added to a 1 M HCl solution no precipitate developed. The content of ethyl alcohol was maintained constant in all aqueous solutions in both the presence and absence of the investigated NI Surf. to eliminate the influence of the ethyl alcohol on the efficacy of the inhibition.

WR technique was done as previously described [30, 31]. PDP measurements were performed by a PS remote potentiostat with PS6 software to estimate the corrosion functions such as steady state (corrosion) potential ($E_{corr.}$), Corrosion current densities ($I_{corr.}$), were obtained by the intersecting of two Tafel lines with ($E_{corr.}$), The electrolytic cell used involves three electrodes e.g., a Pt counter electrode, calomel electrode and CSt as a working electrode. The electrode potential was measured against SCE and it was allowed to stabilize for 30 min. before beginning the tests. A scan rate was set at 2.0 mV s^{-1}. A computer-controlled potentiostat (Auto-Lab 30, Metrohm) was used to execute EIS procedures in a frequency range of 100 kHz to 0.1 Hz with an amplitude of 4.0 mV.

2.2. Synthesis of surfactants molecules

2.2.1. Materials and Methods

IR spectra (υ, cm^{-1}) using KBr were recorded on an FTIR 8300 Shimadzu spectrophotometer. ^{1}H and ^{13}C NMR (δ ppm) spectra were registered with a Bruker AC300 spectrometer (300 MHz for ^{1}H and 75 MHz for ^{13}C) using $CDCl_3$.

*2.2.2. Synthesis of the pyrazoles (**2**, **3**)*

*2.2.2.1. Synthesis of pyrazole (**2**)*

The pyrazole **2** was prepared by adding ethyl cyanoacetate to a hot solution of hydrazide **1** with alcoholic potassium hydroxide for 10 hrs, then the reaction mixture was cooled, and treated by conc. HCl. The solid was filtered and crystallized from EtOH.

*2.2.2.2. Synthesis of pyrazole (**3**)*

The pyrazole **3** was prepared by adding malononitrile to the hydrazide **1** in boiling ethanol with slight drops of piperidine for 5 h. After cooling, the product was filtered and recrystallized from EtOH.

*2.3. Preparation of NI Surf. from the heterocyclic compounds (**I**, **II**)*

NI Surf. **I** and **II** were prepared by adding 5 moles of propylene oxide (P.O) to the pyrazoles (**2**, **3**), respectively [32]. The increasing weight of the mixture after added of P.O is the average amount of propoxylation.

*2.4. Evaluation of the surface-active properties of NI Surf. compounds **I** and **II***

2.4.1. Surface and interfacial tensions

Surface and interfacial tension (γ) were determined using the Du Nouy tensiometer (Kruss K_6) [33] at 25°C.

2.4.2. Critical micelle concentration (CMC)

CMC values were obtained according to [34].

2.4.3. Maximum surface excess Γ_{max}

The maximum surface excess values were measured using the Gibbs equation:

$$\Gamma_{\max} = -\frac{1}{R \cdot T} \cdot \frac{d\gamma}{d \log c}, \quad (1)$$

where, R=8.31×10^7 erg·mol^{-1}·K^{-1}, γ: mN m^{-1}, Γ mol/cm^2, T is absolute temperature, ($d\gamma/d\log C$) is the slope of the [γ against log$C$] plot at 25°C [35].

2.4.4. Minimum surface area (A_{min})

Minimum surface area ($A_{\min}$) was determined from the next relation [36].

$$A_{\min} = \frac{10^{16}}{\Gamma_{\max} \cdot N}, \quad (2)$$

where, N is Avogadro's number, 6.023×10^{23}, and $\Gamma_{\max}$ is the maximum surface excess.

2.4.5. Effectiveness (π_{cmc})

The effectiveness of a certain surfactant π_{cmc} values was measured according to [37] using this equation:

$$\pi_{cmc} = \gamma_0 - \gamma_{cmc}, \quad (3)$$

where γ_0 is the surface tension of the pure water and γ_{cmc} is the surface tension at CMC.

Table 1. Surface functions of the NI Surf. (**I** and **II**).

NI Surf. Compounds	Surface tension (dyne/cm) 0.1 m/l	Interfacial tension (dyne/cm) 0.1 m/l	CMC, mmol/L	Γ_{max}, mol/m^2	π_{cmc}, mN/m	A_{min}, Å
I	38	12	0.90	4.71×10^{-6}	35.00	35.25
II	36	9.5	1.30	4.18×10^{-6}	35.50	39.72

3. Results and Discussion

3.1. Synthesis of azole derivatives (2, 3)

Hydrazide **1** [prepared by treatment of ethyl dodecanoate with hydrazine hydrate] was used for the synthesis of highly substituted pyrazole derivatives. Thus, pyrazole **2** was obtained by refluxing hydrazide **1** with ethyl cyanoacetate in ethanol containing KOH. On the other hand, pyrazole derivative **3** was produced by heating under reflux of hydrazide **1** with malononitrile in ethanol for 4 hrs. Propoxylation of the synthesized pyrazoles (**2**, **3**) with 5 moles of propylene oxide produced NI surfactants **I** and **II**, respectively (Scheme 1).

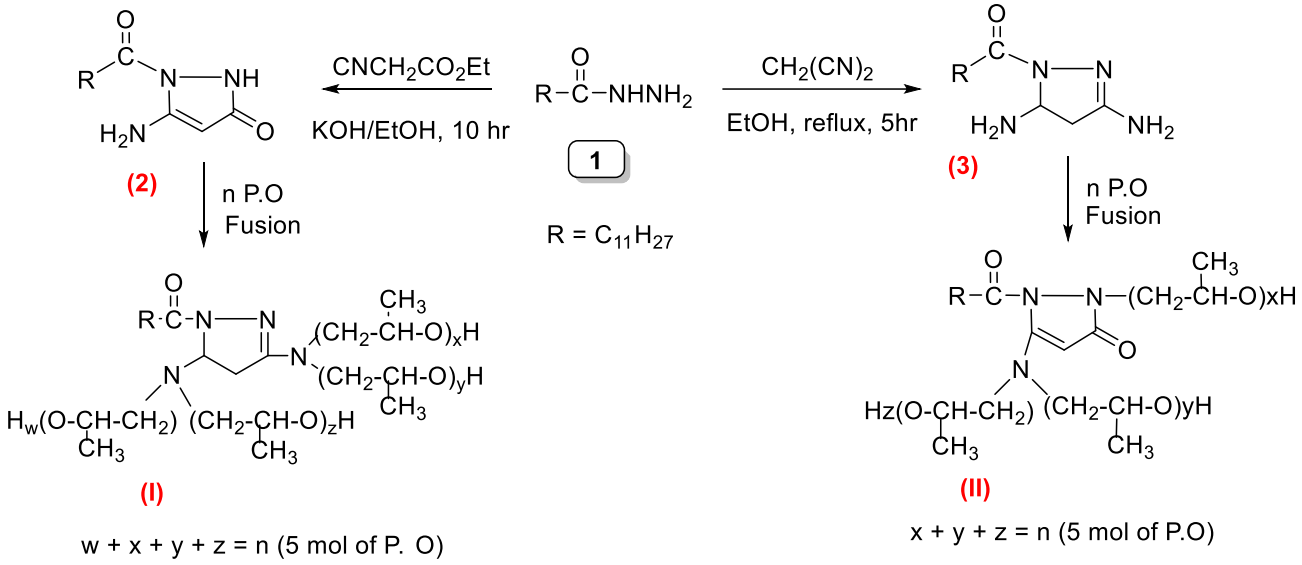

Scheme 1. Synthesis of pyrazole derivatives as nonionic surfactants

The confirmation of the structures of the synthesized compounds was registered in Tables 2 and 3.

Table 2. Physical properties of the synthesized compounds (**2**, **3**).

No.	M.F	M. wt	m.p., °C	Yield, %, Weight, g	Color, Solvent	Analysis data calc./Found, %		
						C	H	N
2	$C_{15}H_{27}N_3O_2$	281.39	155–157	71, 1.51	White, ethanol	64.02 63.83	9.67 9.89	14.93 15.15
3	$C_{15}H_{30}N_4O$	282.25	99–101	76, 1.62	White yellow, ethanol	63.79 64.00	10.71 10.93	19.84 19.60

Table 3. Spectroscopic data for the synthesized NI Surf.

No.	IR, ν/cm^{-1}	^{1}H NMR, δ/ppm	^{13}C NMR, δ/ppm
2	1618 (C=C), 1678 (C=O), 2951, 2848 (CH_2 of the chain), 3318–3141 (NH, NH_2),	0.91 (t, 3H, CH_3), 1.23–1.30 (m, 20H, CH_2), 6.75 (s, 2H, NH_2), 10.35 (s, 1H, NH)	
3	1660 (C=O), 2919, 2849 (CH aliphatic), 3314–3200 (NH_2),	0.99 (t, 3H, CH_3), 1.30–1.27 (m, 20H, CH_2), 1.71 (s, 2H, CH_2 of ring), 3.90 (s, 2H, NH_2), 2.52(s, 2H, NH_2), 6.78 (s, 1H, CH of ring), 7.79 (s, 1H, NH).	14.12, 18.43, 22.69, 25.51, 29.29, 29.31, 29.33, 29.47, 29.60, 31.91, 34.61, 51.48, 152.82, 174.06.
I	960-900, 1170-1100 for C–O–C ether of propoxy chain and 3400–3200 for (OH),	A broad multiple signals appeared at (3.3–3.8) ppm for the propoxy groups.	
II	960-900, 1130-1070 for C–O–C ether of propoxy chain and 3460–3400 for (OH).	A broad multiple signals appeared at (3.1–3.7) ppm for the propoxy groups.	

3.2. PDP study

Figure 1 depicts the PDP curves for CSt in 1 mol/L HCl solution only and also for different concentrations of NI Surf. **I** and **II**. Corrosion functions extracted from the PDP curves such as anodic (β_a), and cathodic (β_c) Tafel slopes, corrosion potential (E_{corr}) corrosion current density (I_{corr}) which are inferred from the intersection of the two straight lines with E_{corr}, and the inhibitory efficacy($\%\eta_{PDP}$) are recorded in Table 4.

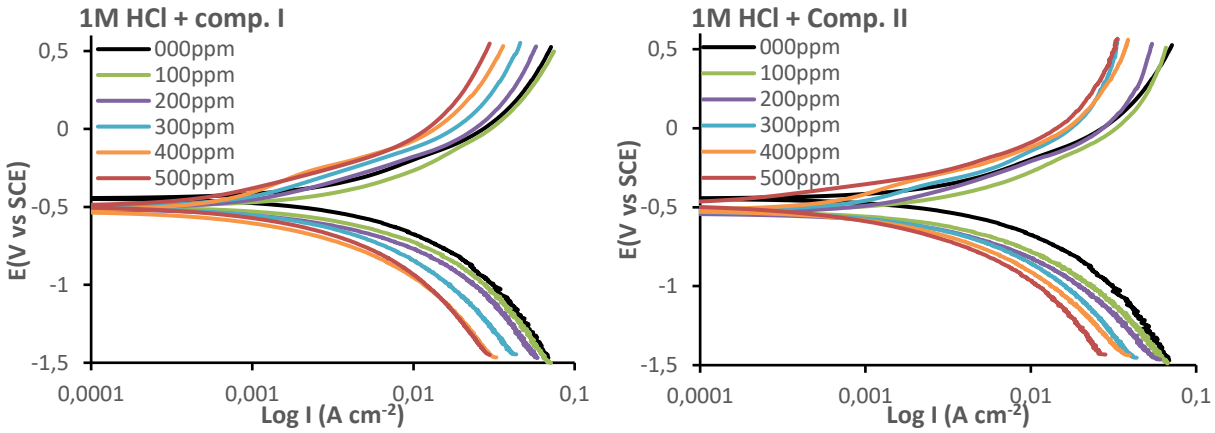

Figure 1. PDP curves for C- steel in 1 mol/L HCl solution alone and when including different concentration of compounds, **I** and **II** at 295K.

$\%\eta_{PDP}$ values can be computed from the next equation:

$$\%\eta_{PDP} = (1 - \frac{I_p}{I_a}) \quad (4)$$

where I_a and I_p are the corrosion current in the acid solution and in the occurrence of some concentrations of NI Surf. **I** and **II** ranged from 100 to 500 ppm. It is apparent from this figure that, with an increase in the concentration of two NI Surf. The anodic corrosion of CSt, and cathodic hydrogen evolution is retarded [38]. PDP curves started with potential approximately constant with rising current indicating simultaneous anodic and cathodic curves until the current moves rapidly into the positive direction (anodic PDP) and in the negative direction (cathodic PDP).

Analysing the data obtained data acquired in Table 4, the variation in E_{corr} (ΔE_{corr}) between the acidic blank solution and contained the two NI Surf. **I** and **II** was less than 85 mV. This suggests that the two NI Surf. compounds are categorized as mixed inhibitors [39, 40]. Two NI Surf. **I** and **II** served by forbidding the active sites on the CSt surface without altering the mechanistic of anodic and cathodic processes. I_{corr} values are minimized and $\%\eta_{PDP}$ increases elucidating the inhibitory impact of NI Surf. **I** and **II**. The inhibitory effect was attributed to the construction of insoluble film caused by the adsorption of NI Surf. compounds on the surface of CSt. The values of $\%\eta_{PDP}$ are 90.41 and 91.76 at 500 ppm NI Surf. compounds **I** and **II**, respectively. At a similar concentration, the $\%\eta_{PDP}$ of compound **II** is more than that of compound **I**.

3.3. EIS method

Nyquist diagrams for CSt electrode in 1 mol/L HCl solution and given concentrations of NI Surf. compounds **I** and **II** (100, 200, 300, 400 and 500 ppm) at 27°C was represented in Figure (2A and 2B). The semicircular manifestation is obtained in the 1 mol/L HCl solution and with some concentrations of NI Surf. compounds demonstrating that the dissolution C-steel electrode in 1 mol/L HCl is principally controlled by the charge transfer operation [41, 42]. The diameter of the capacitive ring augment with augmentation of the concentration of compounds **I** and **II** clarified the reinforcement of adhesive film created on the C-steel surface. The Nyquist diagrams were analyzed by applying the experimental outcomes to a simple equivalent circuit as previously reported [29]. Similar plots were obtained in free in 1 mol/L HCl solution and the inclusion of NI Surf. compounds **I** and **II**. This elucidates that the addition of NI Surf. does not cause a noticeable change in the corrosion process. Corrosion was diminished owing to the increased surface coverage by constructed adsorbent inhibitor layer on the surface of CSt [36–39].

Table 4. Corrosion data was obtained for C-steel in 1 mol/L HCl solution alone and when added various concentrations of NI Surf. **I** and **II** using the PDP method.

Inh.	Inh. conc., ppm	$-E_{corr}$, mV *vs*. SCE	I_{corr}, mA cm^{-2}	$\%\eta_{PDP}$
–	0	443	9.59	–
NI Surf. **I**	100	491	5.02	47.65
	200	472	3.33	65.27
	300	460	2.02	78.93
	400	466	1.42	85.19
	500	465	0.92	90.41
NI Surf. **II**	100	518	4.80	49.95
	200	510	3.12	67.46
	300	494	1.99	79.25
	400	482	1.34	86.03
	400	486	0.82	91.45

The intersection of the half circle with the real component axis yields the charge transfer resistance (R_{ct}). The capacity of double layer (C_{dl}) and inhibitory efficacy from the EIS method ($\%\eta_{EIS}$) were determined from the next equations:

$$2\pi \cdot C_{dl} = \frac{1}{f_{max} R_{ct}} \quad (5)$$

$$\%\eta_{EIS} = (1 - \frac{R_{ct}}{R_{ct,in}}) \cdot 100 \quad (6)$$

where f_{max} is the maximum frequency, and R_{ct} and $R_{ct,in}$ are the charge transfer resistances in 1.0 M HCl solution, and also, in the existence of NI Surf. **I** and **II**, respectively.

The EIS data such as R_{ct}, C_{dl}, and $\%\eta_{EIS}$ are registered in Table 5. Clearly from this table, with increasing concentration of NI. surf compounds the values of R_{ct} are elevated, the C_{dl} depressed and the $\%\eta_{EIS}$ increases. The rise in R_{ct} values originates from the establishment of an adherent film at the CSt surface interface confirming that the dissolution of CSt is under charge transport control [41–43]. The C_{dl} values diminish resulting from the water molecules being substituted by the adsorption of NI Surf. molecules on the C-steel surface. Thus, the corrosion rates are minimized and the $\%\eta_{EIS}$ increases. These outcomes indicate the inhibitory influence of two NI Surf is mainly owing to its adsorption on the CSt surface [36–39].

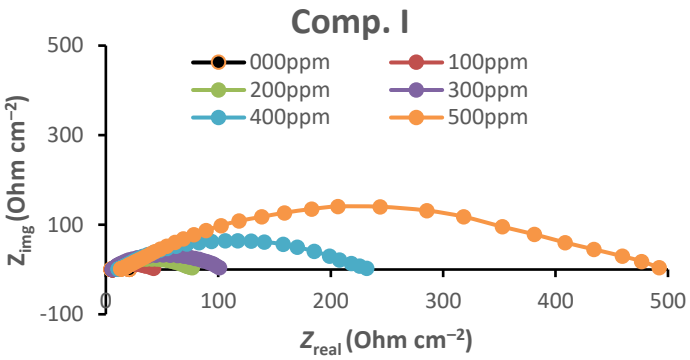

A

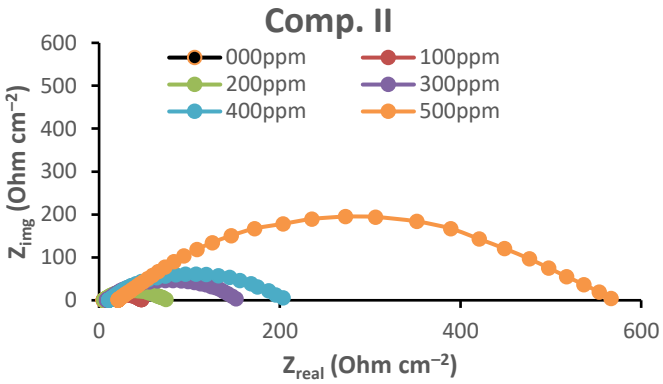

B

Figure 2. Nyquist diagrams for CSt in the free 1 mol/L HCl and when added different concentrations of compounds **I** and **II**.

Table 5. EIS data for CSt corrosion in 1 mol/L HCl solution alone and when combined with varying concentrations of NI Surf. compounds **I** and. **II** at 22°C.

NI Surf. Comp.	NI Surf. Conc., ppm	R_{ct}, Ohm cm^{-2}	C_{dl}	%η_{EIS}
–	0	21.3	12.43	–
Comp. **I**	100	43.9	8.51	53.08
	200	77.4	7.92	73.39
	300	101.9	6.55	79.78
	400	233.2	5.06	91.17
	500	494.6	4.44	95.84

NI Surf. Comp.	NI Surf. Conc., ppm	R_{ct}, Ohm cm^{-2}	C_{dl}	$\%\eta_{EIS}$
Comp. **II**	100	47.7	8.33	56.81
	200	75.2	7.12	72.61
	300	151.4	5.98	86.39
	400	204.8	4.86	89.94
	500	463.9	4.07	96.35

3.4. WR study

3.4.1 Impact of surfactant concentrations

Corrosion rate (R_c) of C-steel electrode in free solution (1 mol/L HCl) and with various concentrations of NI Surf. compounds **I** and **II** in the range100–500 ppm were determined by applying *WR* measurements as displayed in Figure (3A and 3B). It is evident that from this figure, the straight lines were obtained elucidating the deficiency of the insoluble surface film during corrosion. With the concentration of the NI Surf. the *WR* reduces confirming the inhibitory impact of these surfactant compounds.

The corrosion rate (R_C), the inhibitory efficacy ($\%\eta_{WR}$), and the surface coverage (C) of the NI Surf **I** and **II** were computed from the subsequent equations [36–39]:

$$R_C = \frac{\Delta WR}{At} \tag{7}$$

$$\%\eta_{WR} = \frac{R_{c.in}}{R_{c.u}} \cdot 100 \tag{8}$$

$$\Theta = 1 - \frac{R_{c.in}}{R_{c.u}}, \tag{9}$$

where, ΔWR is the variance in *WR*, *A* is the surface area of the CSt sample, *t* is the immersion time in min., $R_{c.u}$ and $R_{c.in}$ is the corrosion rate of CSt in uninhibited of and inhibited solutions, consecutively. ΔWR, $R_{c.}$, Θ and $\%\eta_{WR}$ values were collected in Table 6. From this table it is apparent that with an augmented concentration of NI Surf. the $R_{c.}$ values minimize while the values of Θ and $\%\eta_{WR}$ increase confirming the inhibition power of the NI surfactant **I** and **II**. At a similar concentration of surfactant compounds,the $\%\eta_{WR}$ values of NI Surf. **I** are higher than that of NI Surf. **II**. It is noted that the $\%\eta_{WR}$ values obtained from the three methods (PDP, EIS, and *WR*) utilizing two NI Surf. **I** and **II** are close to each other which shows the accuracy of the obtained results.

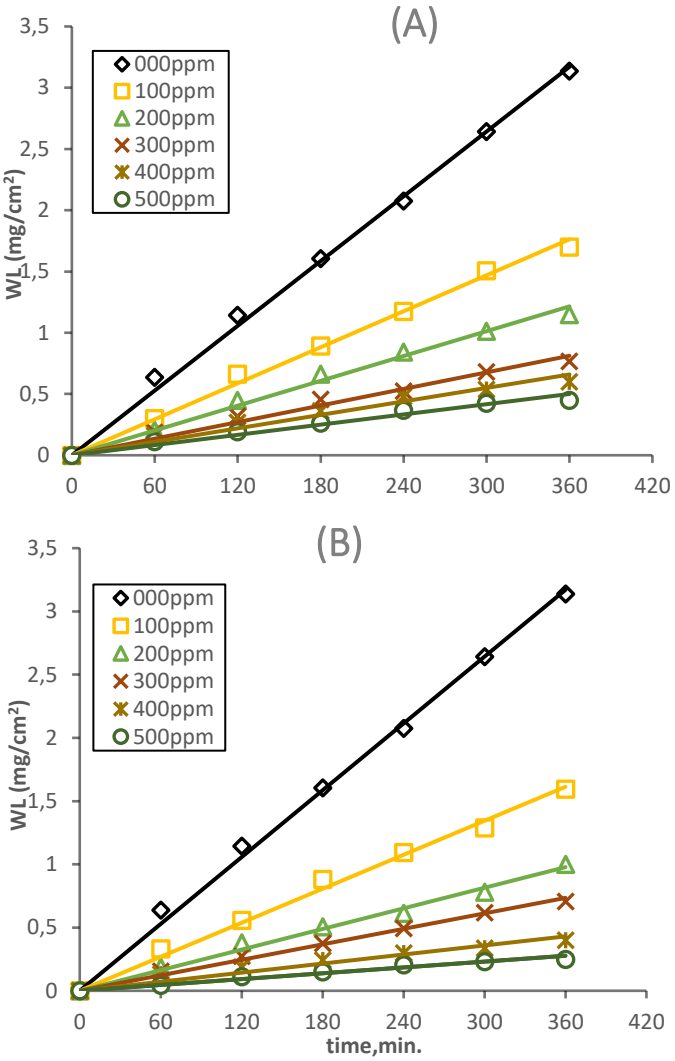

Figure 3. *WR* plots for C-steel in the free 1 mol/L HCl solution and when added different concentrations of (A) NI Surf. **I** and (B) NI Surf. **II** at 22°C.

Table 6. *WR* parameters for CSt in 1 mol/L HCl solution and with vaying concentrations of NI Surf. compounds **I** and **II** at 22°C.

NI Surf.	NI Surf Conc., ppm	ΔWR, mg	$R_c \cdot 10^{-3}$, mg cm^{-2} min^{-1}	Θ	$\%\eta_{WR}$
–	0	50.21	8.715	–	–
Comp. **I**	100	27.24	4.732	0.457	45.70
	200	18.43	3.206	0.632	63.21
	300	12.36	2.151	0.753	75.32
	400	9.02	1.569	0.820	81.99
	500	5.81	1.011	0.883	88.39

NI Surf.	NI Surf Conc., ppm	ΔWR, mg	$R_c \cdot 10^{-3}$, mg cm^{-2} min^{-1}	Θ	%η_{WR}
Comp. **II**	100	25.52	4.350	0.500	50.01
	200	16.07	2.796	0.679	67.91
	300	11.34	1.973	0.774	77.36
	400	6.42	1.117	0.872	87.18
	500	4.82	0.839	0.904	90.37

3.5. Impact of elevated temperature

The impact of temperature rise (22–52°C) on *WR* of CSt in the blank 1 mol/L HCl solution and when including 500 ppm of NI Surf. **I** and **II** were inspected. The same curves in Figure 3 were acquired but not appeared. The outcomes of the corrosion coefficients are listed in Table 7. It is clear from the table that, with elevated temperature the R_c rises while the values Θ and %η_{WR} are minimized. This indicates that the adsorbent layer formed on the surface of CSt is desorbed which led to a decrease in the % η_{WR}. The CSt protection result from the physisorption of the two NI Surf. **I** and **II** onto the surface of the C-steel.

The activation thermodynamics functions the activation energy ΔE_A^*, the enthalpy $\Delta H^*$and the entropy ΔS^* of activation for the dissolution of CSt in a blank 1 mol/L HCl solution and with 500 ppm of NI Surf. **I** and **II**. Were determined from Arrhenius- equation [45–48]:

$$\log R_c = \frac{-E_a}{2.303RT} + \log A \tag{10}$$

$$R_c = \frac{RT}{Nh}\exp(\frac{\Delta S}{R})\exp(-\frac{-\Delta H}{RT}) \tag{11}$$

where *A*, *R*, *h* and *N* are frequency factor, gas constant, Plank's constant and Avogadro's number, respectively.

Table 7. Influence of elevated temperatures on the corrosion parameters of CSt in a blank 1 mol/L HCl and with 500 ppm of NI Surf. **I** and **II**.

	Temp., K	ΔWR, mg	$R_c \cdot 10^{-3}$, mg·cm^{-2}·min^{-1}	%η_{WR}
1.0 M HCl	295	50.23	8.740	–
	305	60.41	10.511	–
	315	69.75	12.136	–
	325	78.60	13.676	–
1.0 M HCl+500 ppm of NI Surf. **I**	295	5.81	1.011	88.39
	305	10.56	1.837	82.52

	Temp., K	ΔWR, mg	$R_c \cdot 10^{-3}$, mg·cm^{-2}·min^{-1}	$\%\eta_{WR}$
1.0 M HCl+500 ppm of NI Surf. **I**	315	18.82	3.274	73.02
	325	27.86	4.847	64.56
1.0 M HCl+500 ppm of NI Surf. **II**	295	4.82	0.839	90.37
	305	8.84	1.538	85.36
	315	14.12	2.457	79.75
	325	21.05	3.663	73.21

Figure 4 describes the relationship between $\log R_c$ *versus* $1/T$ for CSt in blank 1 mol/L HCl solution and when including 500 ppm of NI Surf. **I** and **II**. Straight lines were acquired and from the slope of these lines we set the values of ΔE_A^*. The computed values of ΔE_A^* are equal to 15.40, 36.56 and 40.21 kJ·mol^{-1} for blank 1 mol/L HCl and in the existence of 500 ppm of compound **I** and **II**, respectively. According to several publications, the E_a values for carbon steel corrosion in 1 M HCl are 5.12 kJ·mol^{-1} [47], 4.489 kJ·mol^{-1} [48], 26.82 kJ·mol^{-1} [49], and 19.14 kJ·mol^{-1} [50]. The presence of NI Surf. **I** and **II** led to higher ΔE_A^* values compared to HCl solution alone. This demonstrates that the NI Surf. compounds worked as an inhibitor by rising the values of ΔE_A^* by forming a barrier to mass and charge transfer by adsorbing them on the CSt surface.

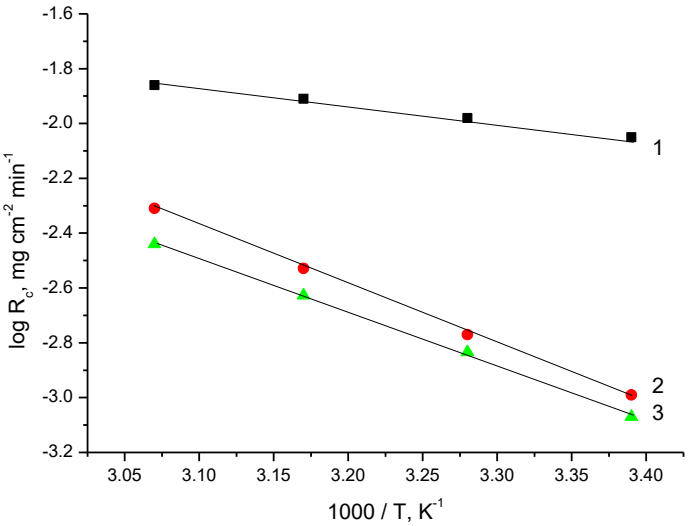

Figure 4. Relationship between $\log R_c$ *vs.* $1/T$ for CSt in blank 1 mol/L HCl solution and when including 500 ppm of NI Surf. **I** and **II**, where 1–1.0 M HCl, 2–1.0 M HCl+500 ppm of NI Surf. **I** and 3–1.0 M HCl+500 ppm of NI Surf. **II**.

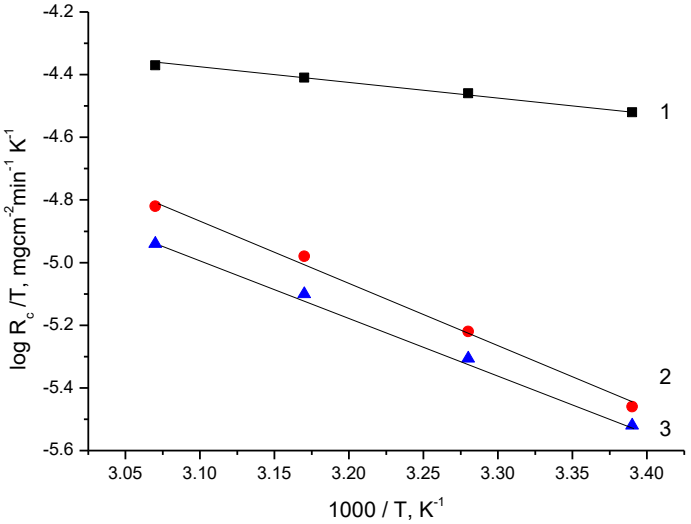

Figure 5. Relationship $\log R_c/T$ *vs.* $1/T$ for CSt in 1 mol/L HCl solution and when including 500 ppm of NI Surf. **I** and **II**, where 1 – 1.0 M HCl, 2 – 1.0 M HCl+500 ppm of NI Surf. **I**, and 3 – 1.0 M HCl+500 ppm of NI Surf. **II**.

Figure 5 presents the correlation between $\log R_c/T$ *versus* $1/T$. Straight lines were acquired in the inhibited and uninhibited solutions. The ΔH^* values were determined from the slope of the straight lines ($-\Delta H^*/2.303R$) and are equal to 11.34, 31.56 and 36.78 for blank 1 mol/L HCl and in the existence of 500 ppm of compound **I** and **II**, respectively. Positive marks of ΔH^* demonstrate that the corrosion of CSt is endothermic. The ΔS^* values were determined from the intercept of the straight lines and equal –156.22 $J \cdot mol^{-1} \cdot K^{-1}$ in blank 1 mol/L HCl solution and equal –248,52 and 359.76 in the existence of 500 ppm of compound **I** and **II**, respectively. The negative marks of ΔS^* demonstrate that the forming of the active complex is an association and not a dissociation step, which means that disorder is reduced during the transition path from the reactants to the activated complex.

3.6. Estimation of surface properties

The surface properties of the NI Surf. **I** and **II** were listed in Tables 1.

3.6.1. Surface tension and interfacial tension

The results showed that the NI Surf. **I** and **II** have high efficiency in decreasing the surface tension as reflected in Table 1, which proved that have clear surface activity.

3.6.2. Critical micelle concentration

The NI Surf. **I** have decrease in CMC value than NI Surf. **II** as outlined in Table 1, which can be attributed to the lower solubility of the surfactant compounds.

3.6.3. Maximum surface excess (Γ_{max})

The results indicated that the increase of Γ_{max} causes to a crowdedness presented at the interface as given in Table 1, which causes a decrease in A_{min} values.

3.6.4. Minimum surface area (A_{min})

All the synthesized surfactants have low A_{min} values. The NI Surf. **I** showed the lowest A_{min} value.

3.6.5. Effectiveness (π_{cmc})

Logically, the efficiency of the surfactants diminishes as (γ_{cmc}) increases as shown in Table 1.

3.7. Inhibition mechanism and adsorption performance

The adsorption of NI Surf. **I** and **II** on the CSt surface are the main step for the inhibition impact of these compounds. The adsorption power is based on the physical and chemical features of the NI Surf. compounds, the sort of metal surface, the corrosive medium and the temperature. Adsorption donates knowledge about the interaction between the adsorbent compounds themselves as well as their reaction with the CSt surface. The adsorption process can be noticed as an exchange operation in which an NI Surf. compounds in the aqueous phase $(\text{NI Surf})_{aq}$, subrogate by "*n*" amount of water molecules adsorbed on the CSt surface to form NI Surf compounds adsorbed on the CSt surface $(\text{NI Surf.})_{ads}$.

$$(\text{NI Surf.})_{aq} + n\text{H}_2\text{O}_{ads} \rightarrow (\text{NI Surf.})_{ads} + \text{H}_2\text{O}_{aq} \quad (19)$$

where *n* is known as the size ratio and is the number of adsorbent water molecules substituted by a single NI Surf. Compound. Adsorption isotherms are mainly utilized to elucidate the adsorption mechanism of NI Surf. on CSt surface. Some isotherms were utilized in this study to choose the suitable isotherm. We found that the Freundlich isotherm is preferable in this work according to the subsequent equation [51]:

$$\log\Theta = \log K_{ads} + n\log C_{\text{NI Surf.}} \quad (20)$$

where $C_{\text{NI Surf}}$. is the concentration of the NI Surf. **I** and **II** compounds used and K_{ads} is the equilibrium constant of adsorption.

Freundlich isotherm diagram ($\log\theta$ *vs.* $\log C_{\text{NI Surf.}}$) for the adsorption of two NI Surf. compounds on the CSt surface in 1.0 M HCl solutions are shown in Figure 6. Straight lines were acquired at the occurrence of the two NI Surf. **I** and **II**. This confirms that the adsorption is subject to Freundlich isotherms.

K_{ads} values were determined from the intercept of the straight lines acquired Langmuir isotherm diagram and equal to $4.8\cdot10^{-1}$ and $4.4\cdot10^{-1}$ for two NI Surf. **I** and **II**, respectively. This elucidates the inhibitory strength of the two NI. Surf. **I** and **II** towards the dissolution of CSt.

The standard free energy of adsorption ΔG°_{ads} was determined by the next equation:

$$55.5K = e^{\frac{\Delta G^{0}_{ads}}{RT}} \quad (21)$$

The value 55.5 is the concentration of water in mol/L. Computed values of ΔG^{0}_{ads} equal to –65.33 and –59.89 kJ mol^{-1} for two NI Surf. **I** and **II**, respectively. Negative values of ΔG^{0}_{ads} elucidate the adsorption of two NI Surf. compounds on the CSt surface are spontaneously and chemically [52].

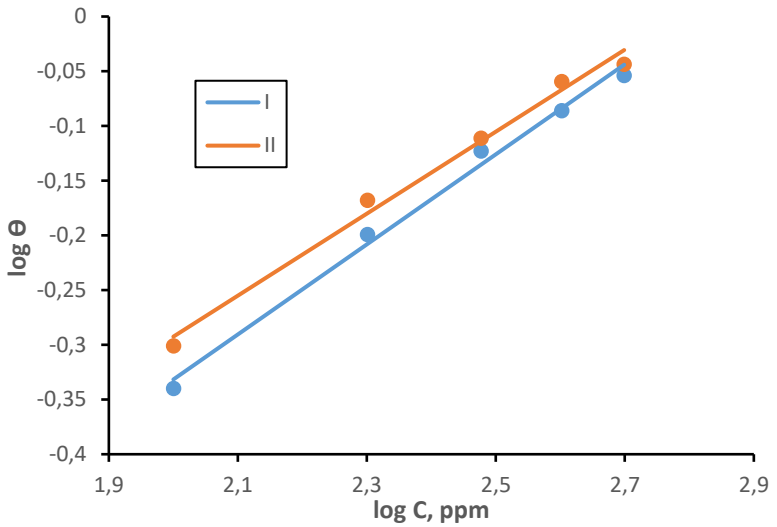

Figure 6. Freundlich isotherm diagram (logΘ vs log$C$) for CSt in 1 mol/L HCl solution with various concentrations of NI Surf. **I** and **II**.

These results are consistent with the surface characteristics of the two NI Surf. **I** and **II** as listed in Table 1. The surface tension, surface tension, and Γ_{max} values are falling while the values for CMC, Γ_{CMC}, and A_{min} are increasing. The protective efficacy of NI Surf. compounds are associated with NI Surf. ability to bind to each other at interfaces and in solution to aggregate to form micelles [53].

The cohesion of surfactant compounds can be determined by the reduction of surface and interfacial tension. The kind of aggregation of surfactant molecules increased the adsorption at the metal surface. The sequence of %η values indicates that the NI Surf **II** is more efficient than NI Surf **II**. These results are consistent with the surface properties of the two compounds as listed in Table 1. The values of values CMC, Γ_{CMC} and A_{min} are increased while the values of surface and interfacial tension and Γ_{max} are reduced which led to the increase of adhesive force between the CSt surface and NI Surf. molecules.

Conclusions

NI Surf. compounds acted as efficacious inhibitors for CSt in 1.0 mol/L HCl.The inhibition efficacy rises with a higher concentration of the surfactant and with a reduction in temperature. Polarization measurements demonstrate that the NI Surf. compounds functioned as mixed inhibitors. The inhibition was interpreted based on the adsorption of NI Surf. compounds on the CSt surface. The adsorption obeys Freundlich isotherm. The surface activity is consistent with the %ηvalues of NI Surf.

Acknowledgment

The authors express their gratitude to Princess Nourah bint Abdulrahman University Researcher supporting project number (PNURSP2023R53). Princess Nourah bint Abdulrahman University, Riyadh, Saudi Arabia.

Conflicts of interests

The authors declare that there are no conflicts of interests regarding the publication of this manuscript.

References

1. N. Insyirah Hairul Salleh and A. Abdullah, Corrosion Inhibition of Carbon Steel Using Palm Oil Leaves Extract, *Indones. J. Chem*., 2019, **19,** no. 3, 747–752. doi: 10.22146/ijc.39707
2. A.S. Al-Gorair, T. Al-Habal, R. El-Sayed, S.S. Al-Juaid, R.S. Abdel Hameed and M. Abdallah, Investigations of non-ionic surfactants derived from triazoles and pyrroles as potent corrosion inhibitors for carbon steel in hydrochloric acid**,** *Int. J. Electrochem. Sci*., 2023, **18**, no. 9, 100269. doi: 10.1016/j.ijoes.2023.100269
3. M. Jeeva, G.V. Prabhu, M. susai Boobalan and C.M. Rajesh, Interactions and Inhibition Effect of Urea-Derived Mannich Bases on a Mild Steel Surface in HCl, *J. Phys. Chem. C*., 2015, **119**, no. 38, 22025–22043. doi: 10.1021/acs.jpcc.5b05788.
4. R. Abdel-Hameed, M.T. Qureshi, M. Abdallah, E. Aljuhani, A.A. Alzharani, A. Alfarsi, A.M. Bakry, B. Huwaimel and O. Farghaly, Recycling of Expired Lactulose Drugs as Eco-Friendly Corrosion Inhibitor for Steel Alloys in Acidic Environment: Gravimetrical and Electrochemical Studies, *Int. J. Electrochem. Sci*., 2022, **17**, no. 12, 221270. doi: 10.20964/2022.12.92
5. R.S. Abdel Hameed, S. Obeidat, M.T. Qureshi, S.R. Al-Mhyawi, E.H. Aljuhani and M. Abdallah, Silver nanoparticles – Expired medicinal drugs waste accumulated at hail city for the local manufacturing of green corrosion inhibitor system for steel in acidic environment, *J. Mater. Res. Technol*., 2022, **21**, 2743–2756. doi: 10.1016/j.jmrt.2022.10.081

6. S. Abd El Wanees, M.G.A. Saleh, M.I. Alahmdi, N.H. Elsayed, M.M. Aljohani, M. Abdelfattah, K.A. Soliman, M.L. Alalati and S.S. Elyan, Benzotriazole-modified chitosan as a controller for the destruction of Al and H_2 generation in the acidic environment, 2024, **311**, 128484. doi: 10.1016/j.matchemphys.2023.128484
7. R.S. Abdel Hameed, E.H. Aljuhani, A.H. Al-Bagawi, A.H. Shamroukh and M. Abdallah, Study of sulfanyl pyridazine derivatives as efficient corrosion inhibitors for carbon steel in 1.0 M H_2SO_4 using analytical techniques, *Int. J. Corros. Scale Inhib*., 2020, **9**, no. 2, 623–643. doi: 10.17675/2305-6894-2020-9-2-16
8. C.M. Fernandes, L.X. Alvarez, N. Escarpini dos Santos, A.C. Maldonado Barrios and E.A. Ponzio, Green synthesis of 1-benzyl-4-phenyl-1H-1,2,3-triazole, its application as corrosion inhibitor for mild steel in acidic medium and new approach of classical electrochemical analyses, *Corros. Sci*., 2019, **149**, 185–194. doi: 10.1016/j.corsci.2019.01.019
9. R.S. Abdel Hameed, A.H. Al-Bagawi, H.A. Shehata, A.H. Shamroukh and M. Abdallah, Corrosion Inhibition and Adsorption Properties of Some Heterocyclic Derivatives on C-Steel Surface in HCl, *J Bio Tribo Corros*, 2020, **6,** 51. doi: 10.1007/s40735-020-00345-y
10. A.S Al-Gorair and M. Abdallah, Expired Paracetamol as Corrosion Inhibitor for Low Carbon Steel in Sulfuric Acid. Electrochemical, Kinetics and Thermodynamics Investigation, *Int. J. Electrochem. Sci*., 2021, **16**, no. 7, 210771. doi: 10.20964/2021.07.73
11. R.S. Abdel Hameed and A.H. Shamroukh, Synthesis, characterization, and evaluation of some acyclic S-nucleosides of pyrazolo[3,4-d] pyrimidine-thiones as corrosion inhibitors for carbon steel in sulfuric acid, *Int. J. Corros. Scale Inhib*., 2017, **6**, no. 3, 333–348. doi: 10.17675/2305-6894 -2017-6-3
12. M. Abdallah, K.A. Soliman, M. Alfakeer, A.M. Al-bonayan, M.T. Alotaibi, H. Hawsawi, O.A. Hazazi, R.S. Abdel Hameed and M. Sobhi, Mitigation effect of natural lettuce oil on the corrosion of mild steel in sulfuric acid solution: chemical, electrochemical, computational aspects, *Green Chem. Lett. Rev*., 2023, **16**, no. 1 2249019. doi: 10.1080/17518253.2023.2249019
13. R.S. Abdel Hameed, M.T. Qureshi and M. Abdallah, Application of Solid Waste for Corrosion Inhibition of Steel in Different Media – *A review*, *Int. J. Corros. Scale Inhib*., 2021, **10**, no. 1, 68–79. doi: 10.17675/2305-6894-2021-10-1-4
14. M. Abdallah, A.S. Al-Gorair, A. Fawzy, H. Hawsawi and R.S. Abdel Hameed, Enhancement of adsorption and anticorrosion performance of two polymeric compounds for the corrosion of SABIC carbon steel in hydrochloric acid, *J. Adhes. Sci. Technol*., 2021, **36**, no. 1, 35–53. doi: 10.1080/01694243.2021.1907041

15. A.S. Al-Gorair, H. Hawsawi, A. Fawzy, M. Sobhi, A. Alharbi, R.S. Abdel Hameed, S. Abd El Wanees and M. Abdallah, Evaluation of the anticorrosion and adsorption properties of polyethylene glycol and polyvinyl alcohol for corrosion of iron in 1.0 M NaCl Solution, *Int. J. Electrochem. Sci*., 2021, **16**, no. 11, 211119, doi: 10.20964/2021.11.03
16. M. Abdallah, K.A. Soliman, R. Alfattani, A.S. Al-Gorair, A. Fawzy and M.A.A. Ibrahim, Insight of corrosion mitigation performance of SABIC iron in 0.5 M HCl Solution by tryptophan and histidine: Experimental and computational approaches, *Int. J. Hydrogen Energy*, 2022, **47**, no. 25, 12782–12797. doi: 10.1016/j.ijhydene.2022.02.007
17. M. Abdallah, F.H. Al-abdali, E.M. Kamar, R. El-Sayed and R.S. Abdel Hameed, Corrosion inhibition of aluminum in 1.0M HCl solution by some nonionic surfactant compounds containing five membered heterocyclic moiety, *Chem. Data Collect*., 2020, **28**, 100407. doi: 10.1016/j.cdc.2020.100407
18. M. Abdallah, A. Fawzy, H. Hawsawi, R.S. Abdel Hameed and S.S. Al-Juaid, Estimation of Water-Soluble Polymers (Poloxamer and Pectin) as Corrosion Inhibitors for Carbon Steel in Acidic Medium, *Int. J. Electrochem. Sci*., 2020, **15**, no. 8, 8129–8144. doi: 10.20964/2020.08.73
19. G. Laadam, M. El Faydy, F. Benhiba, A. Titi, H. Amegroud, A.S. Al-Gorair, H. Hawsawi, R. Touzani, I. Warad, A. Bellaouchou, A. Guenbour, M. Abdallah, and A. Zarrouk, Outstanding anti-corrosion performance of two pyrazole derivatives on carbon steel in acidic medium: Experimental and quantum-chemical examinations, *J. Mol. Liq*., 2023, **375**, 121268. doi: 10.1016/j.molliq.2023.121268
20. R.S. Abdel Hameed, A. El-Zomrawy, M. Abdallah, S.S. Abed El Rehim, H.I. AlShafey and Sh. Nour Edin, Polyoxyethylene stearate of molecular weight 6000 as corrosion inhibitor for mild steel in 2.0 M sulphuric acid, *Int. J. Corros. Scale Inhib*., 2017, **6**, no. 2, 196–208. doi: 10.17675/2305-6894-2017-6-2-8
21. F.H. Al-abdali, M. Abdallah and R. El-Sayed, Corrosion Inhibition of Aluminum using Nonionic Surfactant Compounds with a Six Membered Heterocyclic Ring in 1.0M HCl Solution, *Int. J. Electrochem. Sci*., 2019, **14**, no. 4, 3509–3523. doi: 10.20964/2019.04.59
22. M. Abdallah, H.M. Altass, R. El-Sayed, A.S. Al Gorair, B.A.AL Jahdaly and M. Sobhi, Synthesis and Estimation of Some Surface-Active Compounds Derived from Fused Pyridine as Corrosion Inhibitors for Aluminum in Hydrochloric Acid Solutions, *Prot. Met. Phys. Chem. Surf*., 2021, **57**,811–819. doi: 10.1134/S2070205121040031
23. A. Fawzy, M. Abdallah, M. Alfakeer, H.M. Altass, I.I. Althagafi and Y.A. El-Ossaily, Performance of unprecedented synthesized biosurfactants as green inhibitors for the corrosion of mild steel-37-2 in neutral solutions: a mechanistic approach, *Green Chem. Lett. Rev*., 2021, **14**, no. 3, 488–499. doi: 10.1080/17518253.2021.1943543

24. M. Abdallah, N. El Guesmi, A.S. Al-Gorair, R. El-Sayed, A. Meshabi and M. Sobhi, Enhancing the anticorrosion performance of mild steel in sulfuric acid using synthetic non-ionic surfactants: Practical and Theoretical Studies, *Green Chem. Lett. Rev*., 2021, **14**, no. 2, 382–394. doi: 10.1080/17518253.2021.1921858
25. S.M. Shaban, A.A. Abd Elaal and S.M. Tawfik, Gravimetric and electrochemical evaluation of three nonionic dithiol surfactants as corrosion inhibitors for mild steel in 1M HCl solution, *J. Mol. Liq*., 2016, **216**, 392–400. doi: 10.1016/j.molliq.2016.01.048
26. P. Han, C. Chen, W. Li, H. Yu, Y. Xu, L. Ma and Y. Zheng, Synergistic effect of mixing cationic and nonionic surfactants on corrosion inhibition of mild steel in HCl: Experimental and theoretical investigations, *J. Colloid Interface Sci*., 2018, **516**, no. 15, 398–406. doi: 10.1016/j.jcis.2018.01.088
27. M. Abdallah, T. Al-Habal, R. El-Sayed, M.I. Awad and R.S. Abdel Hameed, Corrosion Control of Carbon Steel in Acidic Media by Nonionic Surfactant Compounds Derived from 1,3,4-Oxadiazole and 1,3,4-Thiadiazole, *Int. J. Electrochem. Sci*., 2022, **17**, no. 12 221255, doi: 10.20964/2022.12.63
28. M. Abdallah, R. El-Sayed, A. Meshabi and M. Alfakeer, Synthesis of Nonionic Surfactants Containing Five Membered Ring: Application as Corrosion Inhibitor of Carbon Steel in 0.5 M H_2SO_4 Solution, *Prot. Met. Phys. Chem. Surf*., 2021, **57**, 389–397. doi: 10.1134/S2070205121010020
29. K. Matsuoka and Y. Moroi, Micellization of fluorinated amphiphiles. *Curr. Opin. Colloid Interface Sci*., 2003, **8**, no. 3, 227–235. doi: 10.1016/S1359-0294(03)00056-6
30. M.J. Rosen, *Surfactant and Interfacial Phenomena*, 3rd Edition, New York, John Willey and Sons, 2004, p. 63.
31. Z. Xu, L. Pengfei, Q. Weihong, L. Zongshi and L. Cheng, Effect of aromatic ring in the alkyl chain on surface properties of aryl alkyl surfactant solution, *J. Surfactants Deterg*., 2006, **9**, no. 3, 245–248. doi: 10.1007/s11743-006-5004-1
32. M. Abdallah, M. Alfakeer, H.M. Altass, A.M. Alharbi, I. Althagafi, N.F. Hasan and E.M. Mabrouk, The polarographic and corrosion inhibition performance of some Schiff base compounds derived from 2-amino-3-hydroxypyridine in aqueous media, *Egypt. J. Pet*., 2019, **28**, no. 4, 393–399. doi: 10.1016/j.ejpe.2019.09.002
33. G. Quartarone, L. Bonaldo and C. Tortato, Inhibitive action of indole-5-carboxylic acid towards corrosion of mild steel in deaerated 0.5M sulfuric acid solutions, *Appl. Surf. Sci*., 2006, **252**, no. 23, 8251–8257. doi: 10.1016/j.apsusc.2005.10.051
34. L.R. Chauhan and G. Gunasekaran, Corrosion inhibition of mild steel by plant extract in dilute HCl medium, *Corros. Sci*., 2007, **49**, no. 3, 1143–1161. doi: 10.1016/j.corsci.2006.08.012
35. M. Abdallah, A. Fawzy and A. Al Bahir, Expired amoxicillin and cefuroxime drugs as efficient anticorrosives for Sabic iron in 1.0M hydrochloric acid solution, *Chem. Eng. Commun*., 2022, **209**, no. 2, 158–170. doi: 10.1080/00986445.2020.1852220

36. M. El Faydy, F. Benhiba, I. Warad, S. Saoiabi, A. Alharbi, A.A. Alluhaybi, B. Lakhrissi, M. Abdallah and A. Zarrouk, Bisquinoline analogs as corrosion inhibitors for carbon steel in acidic electrolyte: Experimental, DFT, and molecular dynamics simulation approaches, *J. Mol. Struct*., 2022, **1265**, 133389. doi: 10.1016/j.molstruc.2022.133389
37. M. Abdallah, K.A. Soliman, M. Alshareef, A.S. Al-Gorair, H. Hawsawi, H.M.Altass, S.S. Al-Juaid and M.S. Motawea, Investigation of the anticorrosion and adsorption properties of two polymer compounds on the corrosion of SABIC iron in 1M HCl solution by practical and computational approaches, *RSC Adv*., 2022, **12**, 20122–20137. doi: 10.1039/D2RA03614B
38. S. Abd El Wanees, A.S. Al-Gorair, H. Hawsawi, M.T. Alotaibi, M.G.A. Saleh, M. Abdallah and S.S. Elyan, Inhibition of pitting corrosion of C-steel in oilfield-produced water using some purine derivatives, *Desalin. Water Treat*., 2022, **269**, 21–32. doi: 10.5004/dwt .2022.28790
39. R.S. Abdel Hameed, M. Alfakeer and M. Abdallah, Inhibiting Properties of Some Heterocyclic Amide Derivatives as Potential Nontoxic Corrosion Inhibitors for Carbon Steel in 1.0M Sulfuric Acid, *Surf. Engin. Appl. Electrochem*., 2018, **54**, 599–606. doi: 10.3103/S1068375518060054
40. S. Bilgiç, Plant Extracts as Corrosion Inhibitors for Mild Steel in HCl Media – Review I, *Int. J. Corros. Scale Inhib*., 2021, **10**, no. 1, 145–175. doi: 10.17675/2305-6894-2021-10-1-9
41. A. Kadhim, A.A. Al-Amiery, R. Alazawi, M.K.S. Al-Ghezi, and R.H. Abass, Corrosion inhibitors. A review, *Int. J. Corros. Scale Inhib*., 2021, **10**, no. 1, 54–67. doi: 10.17675/2305-6894-2021-10-1-3
42. N.K. Gupta, C.S.A. Gopal, V. Srivastava and M.A. Quraishi, Application of expired drugs in corrosion inhibition of mild steel, *Int. J. Pharm. Chem. Anal.*, 2017, **4** no. 1, 8–12. doi: 10.18231/2394-2797.2017.0003
43. A.S. Fouda, M.A. El-Morsy, A.A. El-Barbary and L.E. Lamloum, *Int. J. Corros. Scale Inhib.*, 2016, **5**, no. 2, 112–131. doi: 10.17675/2305-6894-2016-5-2-2
44. M. Abdallah, A. Fawzy and A. Al Bahir, The Effect of Expired Acyclovir and Omeprazole Drugs on the Inhibition of Sabic Iron Corrosion in HCl Solution, *Int. J. Electrochem. Sci*., 2020, **15**, no. 5, 4739–4753. doi: 10.20964/2020.05.86
45. O.L. Riggs and R.M. Hurd, Temperature Coefficient of Corrosion Inhibition, *Corrosion*, 1967, **23**, no. 8, 252–260. doi: 10.5006/0010-9312-23.8.252
46. K.J.Laider, Chemical Kinetics, Mc Graw Hill Publishing Company Ltd., 1965.
47. H.S. Gadow and M. Fakeeh, Green inhibitor of carbon steel corrosion in 1 M hydrochloric acid: Eruca sativa seed extract (experimental and theoretical studies), *RSC Adv*., 2022, **12**, no. 15, 8953–8986. doi: 10.1039/D2RA01296K
48. Raheem A.H.Al-Uqaily, Ruaa Issa Muslim , Subhi A.H. Al-Bayaty , Inhibition by using (ethyl-2-aminothiazole-4-Carboxylate) for copper corrosion in an acidic media, *Egypt. J. Chem*., 2022, **65** no. 10, 403–409. doi: 10.21608/EJCHEM.2022.110271.5018

49. M. Salah, L. Lahcène, A. Omar and H. Yahia, Study of corrosion inhibition of C38 steel in 1 M HCl solution by polyethyleneiminemethylene phosphonic acid, *Int. J. Ind. Chem*., 2017, **8**, 263–272. doi: 10.1007/s40090-017-0123-2
50. A.Thomas, M. Prajila, K.M. Shainy and A. Joseph, A green approach to corrosion inhibition of mild steel in hydrochloric acid using fruit rind extract of Garcinia indica (Binda), *J. Mol. Liq*., 2020, **312**, 113369. doi: 10.1016/j.molliq.2020.113369
51. M. Abdallah, H.M. Al–Tass, B.A. AL Jahdaly and A.S. Fouda, Inhibition properties and adsorption behavior of 5-arylazothiazole derivatives on 1018 carbon steel in 0.5M H_2SO_4 solution, *J. Mol. Liq*., 2016, **216**, 590–597. doi: 10.1016/j.molliq.2016.01.077
52. M. Sobhi, R. El-Sayed and M. Abdallah, The Effect of Non Ionic Surfactants Containing Triazole, Thiadiazole and Oxadiazole as Inhibitors of the Corrosion of Carbon Steel in 1M Hydrochloric Acid, *J. Surfactants Deterg*., 2013, **16**, no. 6, 937–946. doi: 10.1007/s11743-013-1468-y

♦ ♦ ♦